IEEE Access
Multidisciplinary | Rapid Review | Open Access Journal

Received June 16, 2019, accepted June 25, 2019, date of publication June 27, 2019, date of current version July 25, 2019.

Digital Object Identifier 10.1109/ACCESS.2019.2925470

Optimal Sliding Mode Chaos Control of Direct-Drive Wave Power Converter

JUNHAO HUANG, JUNHUA YANG, DONGSHEN XIE, AND DANQI WU
School of Automation, Guangdong University of Technology, Guangzhou 510006, China

Corresponding author: Junhua Yang (yly93@gdut.edu.cn)

This work was supported in part by the National Natural Science Foundation of China under Grant 513770265, and in part by the Natural Science Foundation of Guangdong Province under Grant 2016B090912006 and Grant 2015A030313487.

ABSTRACT In this paper, in order to investigate the chaos control problem of direct-drive wave power conversion system, the hydrodynamic model of Archimedes wave swing and the state equation of permanent magnet linear synchronous motor are analyzed, and a decoupling mathematical model of the wave power converter is built in combination with feedback decoupling system. The maximum Lyapunov exponent spectrum is used to verify the chaotic phenomenon of the direct-drive wave power converter, and the dynamic response of the converter when entering the chaotic state is explored. A composite sliding mode chaotic controller is proposed. Based on the BP neural network, the global effect of the control parameters is fitted, and the particle swarm optimization algorithm is adopted to optimize the parameters of sliding mode control to determine the optimal control parameters. The Lyapunov criterion is used in stability analysis to prove the effectiveness of the control strategy. The simulation reveals that the sliding mode control strategy can disengage the wave power converter from the chaotic state to the stable state. With particle swarm optimization, the strategy can shorten the response time, suppress the overshoot and enhance system robustness.

INDEX TERMS Direct-drive wave power converter, chaos control, sliding mode control, particle swarm optimization, parameter optimization.

I. INTRODUCTION

As one of the renewable clean energy sources, wave energy exhibits high power density and enjoys large reserves, which can satisfy 10% of global electricity demand through its effective utilization [1]. Wave energy converters (WEC),capable of converting wave energy into electrical energy, primarily consist of pendulum type, point suction type, oscillating water column type, water valve type as well as direct drive type [2]. In Ref. [3], the structural characteristics of Archimedes wave swing (AWS) and the process in wave energy conversion were introduced. In Ref. [4], [5], the types of motors suitable for AWS were explored. By analyzing the operating characteristics, it was highlighted that, permanent magnet linear synchronous motors (PMLSM) outperform rotating motors in energy conversion. Besides, the mover of PMLSM can follow the wave to move linearly. Therefore, when PMLSM is adopted for WEC, the intermediate conversion device can be omitted, thereby significantly enhancing conversion efficiency [6], [7]. The direct-drive wave power system, consisting of AWS and PMLSM, is capable of efficiently converting wave energy into electrical energy, which has been extensively studied [8]–[10]. Based on the PID control strategy, the stable control can be achieved for the direct drive wave power system [11], [12]. In Ref. [13], a novel optimum PI controller was introduced to control the current of the generator, and the transient stability of the WEC system coupled by AWS and PMLSM was enhanced. In Ref. [14], a gravitational search algorithm was adopted to enhance the stability of the WEC system by controlling the d and q axis currents of the generator.

According to the study, in the case of specific parameters, the current, the speed and the torque of the permanent magnet synchronous motor will display short-time violent oscillation, irregular noise will be generated and the motor will be hard to control. These phenomena are termed as chaotic state [15]–[17]. In Ref. [18], it was verified that the system is likely to appear chaotic state when there exist chaotic attractors. Due to the unstable and unpredictable input of the WEC and highly uncertain external environment, PMLSM, a strongly coupled complex motor system, can be in the chaotic state more easily [19]. When the motor is in a chaotic

The associate editor coordinating the review of this manuscript and approving it for publication was Sun Junwei.

state, the normal operation of the entire wave power generation system and grid connection will be directly affected for the severe instability of the motor. Accordingly, the chaotic characteristics of WEC requires exploration and the method to achieve WEC chaos detachment and stable control should be developed.

At low speeds, the chaotic control of the PMLSM can be achieved by optimizing the design of the stator core, winding, rotor permanent magnet as well as other motor structures [20]. In Ref. [21], a high-speed chaotic controller was put forward, achieving chaotic control of the generator system in accordance with the stability theory of the three-diagonal structure matrix. Such controller is capable of shortening the transient time by increasing the value of the control parameters. In Ref. [22], the PMLSM model was converted into a Lorentz-like model and an active disturbance rejection control (ADRC) strategy was adopted to suppress the chaotic phenomenon of the motor and solve the problem of unknown parameter. In Ref. [23], extended state observers were used to optimize the effect of sliding mode control strategy, so that the target system can reach stable in the case of unknown partial states and upper limit of the nonlinear uncertainties. In Ref. [24], the non-singular fast-terminal sliding mode chaos control method was employed to suppress the chaotic phenomenon of the PMLSM and reduce the dependence on the speed sensor. In Ref. [25], an adaptive sliding mode control strategy was formulated to detach PMLSM from chaotic state under uncertain parameters. Nevertheless, the change of control parameters in sliding mode control will have a great impact on the control effect. Thus, it has been a hot spot to find the optimal control parameters to optimize the control effect. In Ref. [26], to capture the maximum power for wind turbines, the particle swarm optimization algorithm was adopted to the sliding mode control to optimize control parameters. When the chaotic system has multiple undetermined parameters, the feasibility of the control strategy will be reduced. The synchronization of chaotic systems with unknown parameters can be achieved in a finite time by adopting the sliding mode control strategy in accordance with finite time stability theory and adaptive control principle [27], [28]. However, the existing chaos researches primarily focused on the motor, but did not consider the chaotic characteristics and control strategy of the entire WEC system.

In this paper, the WEC chaotic mathematical model was built, and the WEC chaotic characteristics were analyzed. Based on the above analysis, the sliding mode control strategy combined with artificial intelligence algorithm was designed to achieve stable control and optimize the control effect. The simulation on the MATLAB / Simulink platform reveals that the designed optimal control strategy is capable of quickly detaching the target system from chaotic state, achieving stability and enhancing system robustness.

This paper is organized as follows. The AWS hydrodynamic model and the PMLSM mathematical model were built, and the state feedback decoupling was used to yield the decoupling WEC mathematical model based on d-q axis

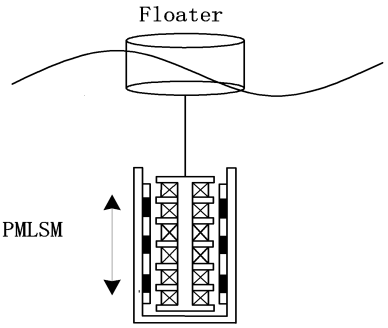

FIGURE 1. The structure of WEC.

in Section II. The Lyapunov exponent spectrum was employed to verify the chaotic phenomenon in WEC, and the current and velocity response of WEC in chaotic state were analyzed in Section III. In Section IV, a sliding mode controller was proposed for WEC chaos detachment. BP neural network was adopted to fit the global control effect of different control parameters. Subsequently, the PSO algorithm is used to optimize the control parameters to obtain the optimal control parameters. The simulation verified the effect of sliding mode controller in Section V. Lastly, a conclusion was drawn in Section VI.

II. MATHEMATICAL MODEL OF WEC

The structure of WEC is shown in Fig. 1. The WEC consists of a wave energy capture device and a wave energy conversion device. The AWS is moved by the external wave force to drive the mover of PMLSM to reciprocate linearly, thus cutting the magnetic induction line, and then generating an induced potential in the stator winding.

A. THE HYDRODYNAMIC MODEL OF AWS

Assuming that the input wave is a sine wave, when the AWS is subjected to wave forces, the displacement and velocity formula of the floater are expressed as follows:

$$\begin{cases} x = Xsin\,(\omega t) \\ v = \dfrac{dx}{dt} = Vsin\,(\omega t) \end{cases} \tag{1}$$

where X and V are the displacement and velocity peak of floater, respectively, and ω is the wave frequency.

When the wave input acts on the floater, the floater will oscillate and rotate with the wave motion. Since the linear motor can only absorb the vertical motion, only the single-degree-of-freedom force analysis is performed.

When the floater is in a static equilibrium state, the static buoyancy F_h is defined as:

$$F_h = -\rho g S x = -K_s x \tag{2}$$

where ρ is the density of seawater, g is the acceleration of gravity, S is the cross-sectional area of the cylindrical surface, and the equivalent elastic coefficient $K_s = \rho g S$.

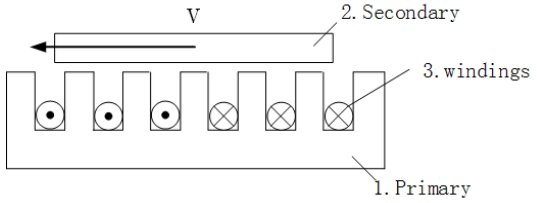

FIGURE 2. The structure of PMLSM.

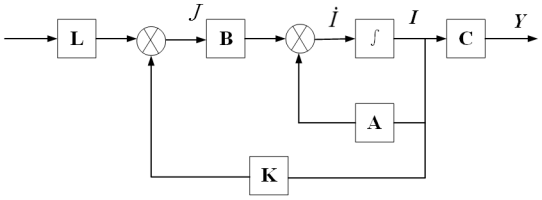

FIGURE 3. State feedback decoupling.

When the floater is subjected to a wave force, a vertical wave force F_d will be generated, which is expressed as:

$$F_d = -\rho g S_0 K_p(\omega, h, d) C(\omega) \tag{3}$$

where S_0 denotes the surface area of floater immersed in sea, h is the depth of the sea surface, d is the distance from the float to the sea level, C is the peak value of the ocean wave, and K_p is the pressure coefficient of the float, which is related to the wave frequency, wave height and depth.

When the floater is subjected to a wave force, the floater receives the radiation force F_r, which is:

$$F_r = -A\ddot{x} - B\dot{x} \tag{4}$$

where A is the additional quality and B is the radiation damping coefficient.

The wave force acting on the floater is defined as:

$$F_{wave} = F_h + F_d + F_r \tag{5}$$

In accordance with Newton's second law, the motion equation is written as:

$$M_f\ddot{x} = F_{wave} + F_g \tag{6}$$

where M_f denotes the quality of floater and F_g is the force exerted by the linear motor to the floater.

B. THE CHAOTIC STATE EQUATION OF PMLSM

The structure of PMLSM is illustrated in Fig. 2. The Primary of PMLSM is fixed, while the secondary can perform linear motion. Unlike the rotating motor, the motion track of the PMLSM mover is a straight line, and the permanent magnets are alternately distributed on the moving path. When passing through the three-phase sinusoidal alternating current, a traveling wave magnetic field will be generated, in which the direction is opposite to the moving direction of the mover.

To establish a mathematical model of PMLSM, suppose:

(1) The iron core of PMLSM is not saturated;

(2) Only the fundamental magnetic potential is considered;

(3) No damper winding is installed on the mover;

(4) Ignore the eddy current loss [29].

Given the edge effect of PMLSM, the chaotic mathematical model of PMLSM is derived from Parker transformation and radiation transformation [25]:

$$\begin{cases} \dot{i}_d = -i_d + i_q v + \hat{u}_d \\ \dot{i}_q = -i_q + \delta i_d v + \gamma v + \hat{u}_q \\ \dot{v} = \delta\left(i_q - v\right) - F_f \end{cases} \tag{7}$$

where, u_d, u_q, i_d, i_q denote d-q axis voltage, current, v is speed of linear motor mover, F_f is motor load resistance, $\hat{u}_d = \frac{1}{R_s k}u_d$, $\hat{u}_q = \frac{1}{R_s k}u_q$, $\tau = \frac{L_q}{R_s}$, $F_f = \frac{\tau^2}{M}F_g$, $k = \frac{2BR_s\tau}{3L_q\pi\psi}$, $\delta = -\frac{\pi}{\tau_n}$, $\gamma = -\frac{\psi_f}{kL_q}$, $\sigma = \frac{B\tau}{M}$, L_d, L_q are d-q axis inductance, τ_n is the linear motor pole pitch, R_s is the primary phase resistance, M is the quality of secondary, B is the viscosity coefficient, and ψ is the motor flux.

Ignore the superscript in (7) and combine with the equation (6), the simplified expression is:

$$\begin{cases} \dot{i}_d = -i_d + i_q v + u_d \\ \dot{i}_q = -i_q + \delta i_d v + \gamma v + u_q \\ \dot{v} = \sigma\left(i_q - v\right) - K_g\left(M_f\ddot{x} - F_{wave}\right) \end{cases} \tag{8}$$

C. DECOUPLING MATHEMATICAL MODEL OF WEC

According to equation (8), WEC is hard to control directly because of the couple between d-q axis current, which makes decoupling necessary. Using state feedback decoupling as shown in Fig. 3, a decoupling matrix is established to achieve decoupling of equation (8) [30].

$$\begin{cases} \dot{I} = AI + BJ \\ Y = CI \\ L = \left(CA^0B\right)^{-1} \\ K = -AB^{-1} \end{cases} \tag{9}$$

where $A = \begin{bmatrix} -1 & V \\ \sigma V & -1 \end{bmatrix}$, $B = \begin{bmatrix} 1 & 0 \\ 0 & 1 \end{bmatrix}$, $C = \begin{bmatrix} 1 & 0 \\ 0 & 1 \end{bmatrix}$, $I = \begin{bmatrix} i_d \\ i_q \end{bmatrix}$, $U = \begin{bmatrix} u_d \\ u_q + \gamma v \end{bmatrix}$.

Combining equations (8) and (9), the chaotic decoupling mathematical model of PMLSM is obtained.

$$\begin{cases} \dot{i}_d = u_d^* \\ \dot{i}_q = \gamma v + u_q^* \\ \dot{v} = \sigma\left(i_q - v\right) - -K_g\left(M_f\ddot{x} - F_{wave}\right) \end{cases} \tag{10}$$

After the above changes, the system order changes from 3 to 2. Then, the d-q axis decoupling control of the WEC has been completed.

III. CHAOTIC ANALYSIS OF WEC

A. CHAOTIC IDENTIFICATION OF WEC

Chaos recognition is a key step in chaos analysis. The Lyapunov exponent has been the most commonly used method for chaos criterion. For a chaotic system, in the case of a slight change in the initial value, it is likely to cause the

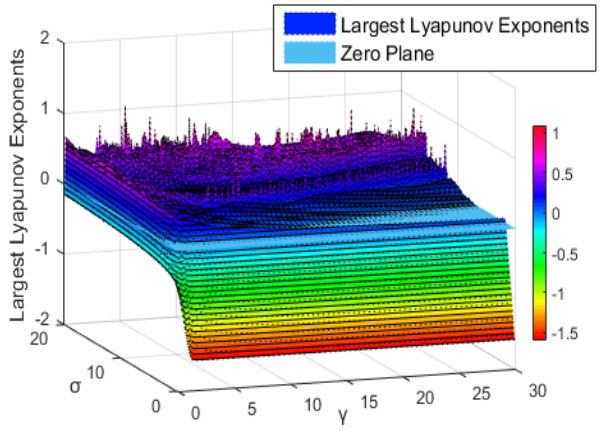

FIGURE 4. The maximum Lyapunov exponent of WEC.

two motion tracks to gradually exponentially grow apart and enter a chaotic state. The Lyapunov exponent can accurately reflect the average divergence index rate of the motion track in the chaotic system due to the initial difference. Lyapunov exponent of the system below 0 indicates that the system phase volume is shrinking and inclined to be stable. In contrast, when the system Lyapunov exponent above 0, the system phase volume will increase, and the motion track will gradually separate and eventually reach the chaotic state. Therefore, when the Lyapunov exponent of a chaotic system exhibits at least one positive value, the system will be in the chaotic state. The specific performance refers to the boundedness and randomness of the system's motion track in a certain area [31], [32]. Through calculating the maximum Lyapunov exponent of the system and determining the positive and negative values, the system state can be judged.

The Wolf algorithm can track the distance change Δd of the motion track of two points over time, if Δd increases with time, the system will reach the chaotic state [33]. The Δd calculation is define as:

$$\Delta d_{max} = \lim_{n\to\infty} \frac{1}{n\lambda} \sum_{i=1}^{n} ln\left(\frac{d_i}{d_0}\right) \tag{11}$$

where λ is the integral step size and d_0 is the initial distance of the two points of motion.

B. CHAOTIC ANALYSIS OF WEC

Based on Matlab/Simulink, the simulation model is built to explore the chaotic phenomenon of WEC basing on the decoupling mathematical model. When the parameters σ and γ take different values, the maximum Lyapunov exponent will be calculated, and the simulation results are shown in Fig. 4.

According to Fig. 4, with the value change of σ and γ, the maximum Lyapunov exponent changes constantly. Besides, the parameter σ has a larger impact on this value. When parameter σ gradually decreases to about 5, the maximum Lyapunov exponent gradually turns to a negative value and passes the zero plane, and the system is disengaged from the chaotic state.

The PMLSM parameters are as follows:d and q-axis inductance L_d and $L_q$are 0.07H, the primary phase resistance R_s is 0.2 Ω, the linear motor pole pitch τ_n is 1m, the motor flux ψ is 0.46Wb, the quality of floater M_f is 50kg and the quality of secondary M is 40kg. Based on Matlab/Simulink, the d-q axis current and speed of WEC under chaotic state are explored. The result is shown in Fig. 5.

As shown in Fig. 5, it can be seen that the d-q current and speed of WEC oscillate within a certain range.

IV. DESIGN AND OPTIMIZATION FOR SLIDING MODE CONTROL OF WEC

A. CONTROLLER DESIGN

The sliding mode control aims to design the sliding surface and control rate according to the target value of the target system, then the motion track of the system will move to the sliding surface designed by sliding mode controller. The effect of sliding mode control is affected by system parameters, instead of by external fluctuations,which makes the control robust.

According to equation (10), controlling the d and q axis voltages can control the d-axis current, the q-axis current, and the speed, respectively. Set i_d^* and v^* as the target values of i_d and v, respectively. In order to reduce the WEC power loss, the target value of i_d is usually determined as 0, and the target value of v is determined by the input wave.

Define target value error e_d and e_v, so the tracking error equation is:

$$\begin{cases} e_d = i_d - i_d^* \\ e_v = v - v^* \end{cases} \tag{12}$$

The derivative of equation (12) is:

$$\begin{cases} \dot{e}_d = \dot{i}_d = u_d^* \\ \dot{e}_v = \dot{v} - \dot{v}^* \end{cases} \tag{13}$$

Define $u_d^* = a(t) + \Delta$,where Δ is external disturbance. Design the sliding mode controller for e_d:

$$s_d = \dot{e}_d - c_1 e_d = u_d^* - c_1 e_d \tag{14}$$

where c_1 is the control parameter, and c_1 greater than zero. And the derivative of equation (14) is:

$$\dot{s}_d = \dot{u}_d^* - c_1 \dot{e}_d = a(t) + \Delta - c_1 u_d^* \tag{15}$$

Constructing a Lyapunov function for equation (15):

$$\lambda_d = \frac{1}{2} s_d^2 \tag{16}$$

The derivative of equation (16) is:

$$\dot{\lambda}_d = s_d \dot{s}_d = s_d \left(a(t) + \Delta - c_1 u_d^*\right) \tag{17}$$

Design the sliding control rate:

$$a(t) = -k_1 s_d - \eta_1 sgn(s) + c_1 u_d^* \tag{18}$$

where $k_1 > 0, \eta_1 > 0$.

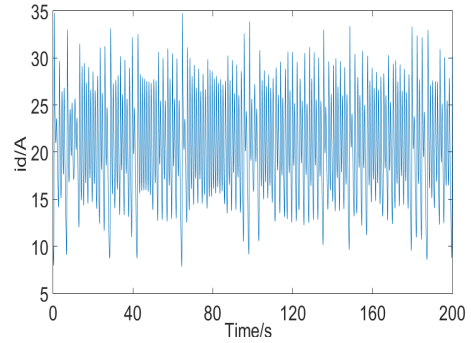

(a) The d-axis current under chaotic state

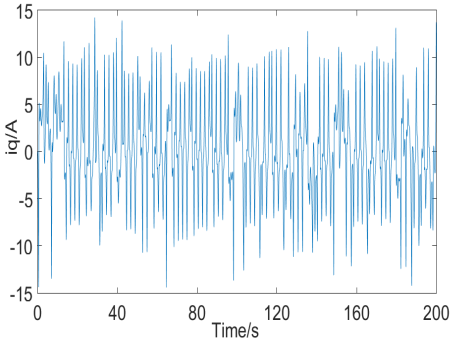

(b) The q-axis current under chaotic state

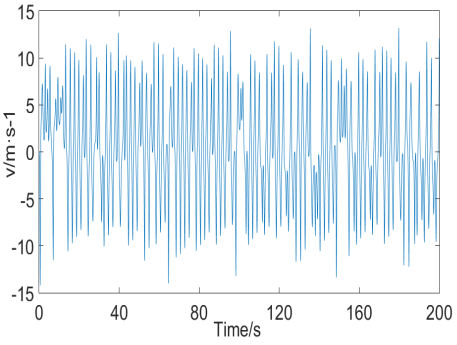

(c) The speed under chaotic state

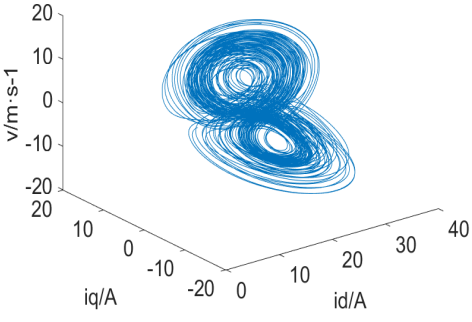

(d) The trajectory of WEC under chaotic state

FIGURE 5. Chaotic state of WEC when $\sigma = 10$ and $\gamma = 15$.

Substituting equation (18) into (17), calculation shows $\dot{\lambda}_d = s_d \dot{s}_d \leq -\eta_1 |s_d| - k_1 s_d^2 < 0$.Therefore, the control rate of u_d can control the d-axis current of the WEC.

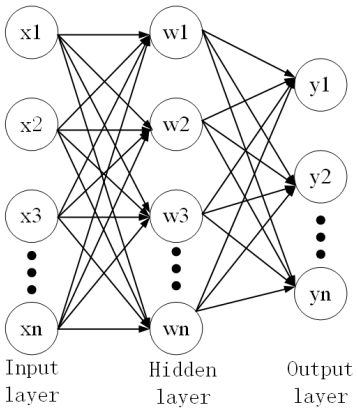

FIGURE 6. The structure of BP neural network.

Define $\ddot{e_v} = v(t) + b(t)$, where $v(t)$ is the function about motor speed, which is influenced by input wave. Design the sliding mode controller for e_v:

$$s_v = \dot{e}_v - c_2 e_v \tag{19}$$

where c_2 is the control parameter, and c_2 greater than zero. The derivative of equation (19) is:

$$\dot{s}_v = \ddot{e}_v - c_2 \dot{e}_v = v(t) + b(t) - c_2 \left(\dot{v} - \dot{v}^*\right) \tag{20}$$

Constructing a Lyapunov function for equation (20):

$$\lambda_v = \frac{1}{2} s_v^2 \tag{21}$$

The derivative of equation (21) is:

$$\dot{\lambda}_v = s_v \left(v(t) + b(t) - c_2 \left(\dot{v} - \dot{v}^*\right)\right) \tag{22}$$

According to equation (22), design the sliding control rate:

$$b(t) = -k_2 s_v - \eta_2 sgn(s) - v(t) - c_2 \dot{v} + c_2 v^* \tag{23}$$

where $k_2 > 0$, $\eta_2 > 0$.

Substituting equations (23) into (22), calculation shows $\dot{\lambda}_v = s_v \dot{s}_v \leq -\eta_2 |s_v| - k_2 s_v^2 < 0$.Therefore, the control rate of v can control the speed and q-axis current of the WEC.

Above all, the sliding mode controller for WEC is completed.

B. BP NEURAL NETWORK FITTING GLOBAL EFFECT OF CONTROL PARAMETERS

According to equation (18) and (22), there are six changeable parameters: c_1,k_1,η_1,c_2,k_2,η_2. Based on the simulation calculation, η_1 and η_2 have little influence on the control effect, but the little changes of the other four parameters will affect the response time and overshoot significantly.

BP neural network is an artificial intelligence technology emerging in recent years. The structure of BP neural network is shown in Fig. 6. Due to the strong learning approximation ability of the BP neural network, fitting to any nonlinear function can be achieved. BP neural network is used to explore the effect of response time and overshoot when control parameters change. The process of fitting has three steps:

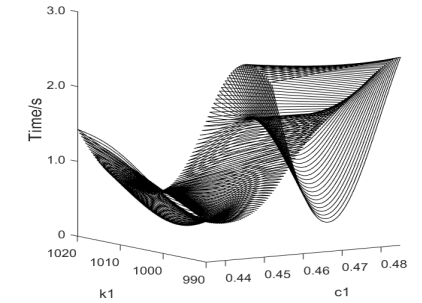

(a) Response time of d-axis current

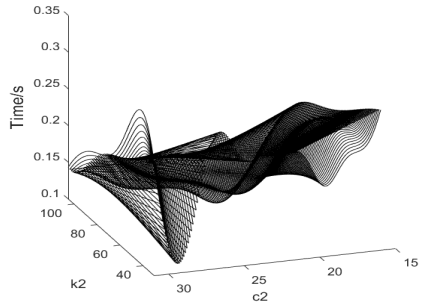

(b) Response time of q-axis current

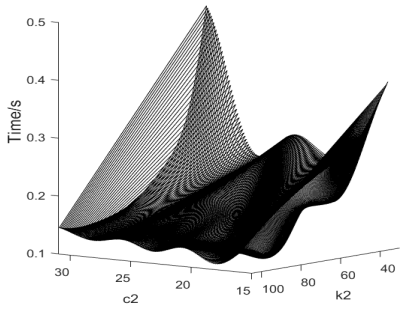

(c) Response time of speed

FIGURE 7. Response time of WEC when $\sigma = 10$ and $\gamma = 15$.

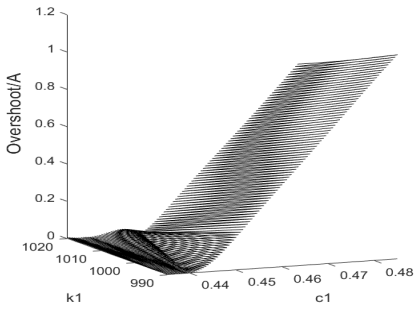

(a) Overshoot of d-axis current

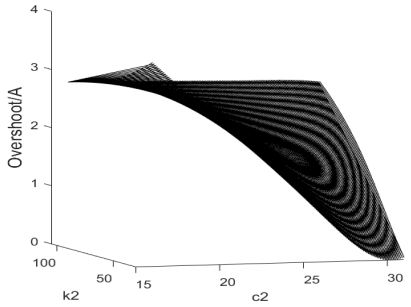

(b) Overshoot of q-axis current

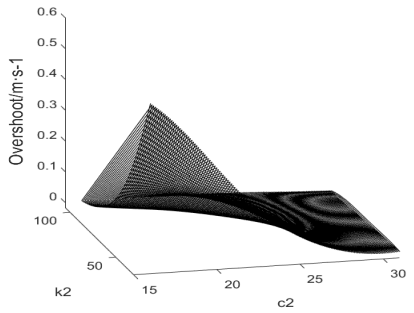

(c) Overshoot of speed

FIGURE 8. Overshoot of WEC when $\sigma = 10$ and $\gamma = 15$.

(1) Construct the BP network;
(2) Train the BP network;
(3) Use the trained network to predict the response time and overshoot.

The result is illustrated in Fig. 7 and Fig. 8.

As shown in Fig. 7 and Fig. 8, the response time and overshoot vary greatly in case of different control parameters, which leads to multiple local optimum values. The conventional empirical method can be used to determine the parameters with good control effect, whereas it cannot determine the parameters with the optimal control effect.

C. PSO OPTIMIZES SLIDING MODE CONTROL PARAMETERS

Particle Swarm Optimization (PSO) is a bionic algorithm that simulates population foraging. It exhibits a fast search speed and can find the optimal solution promptly. Thus it has been widely used in the optimization problem of industrial control field [34]. The PSO position and speed update are expressed as follows:

$$\begin{cases} v_{i+1} = \theta v_i + c_a r(p_{best} - x_i) + c_b r(g_{best} - x_i) \\ x_{i+1} = x_i + v_{i+1} \end{cases} \tag{24}$$

where θ denotes the inertia weight, c_a and c_b are the learning rates, r is a random number between 0 and 1, x_i is the position of i-th particle , v_i is the motion velocity of i-th particle , and p_{best} and g_{best} refer to the particle history optimal position and the particle group history optimal position, respectively. The PSO workflow is shown in Fig. 9.

The purpose of optimization is to shorten the response time and suppress the overshoot.

According to equation (10), PMLSM system has achieved d-q axis decoupling. Accordingly, the control for the d-axis and the q-axis has been separated and independent on each

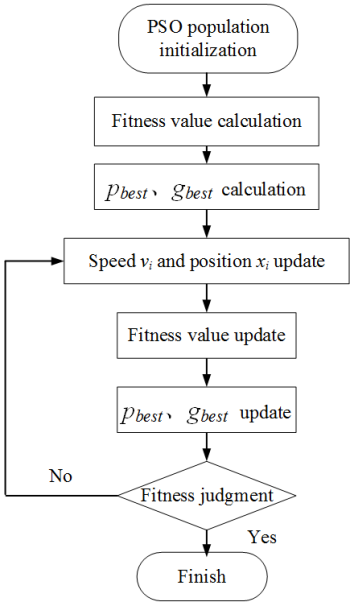

FIGURE 9. The PSO workflow.

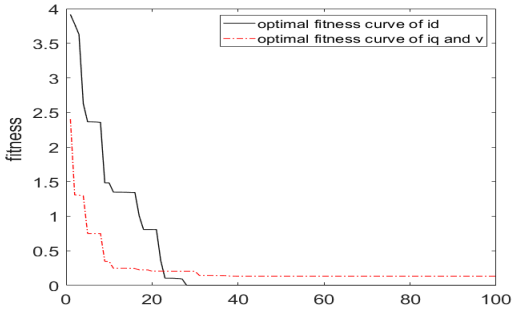

FIGURE 10. The fitness curve.

other. Therefore, the fitness function is set as follows:

$$\begin{cases} f_d = T_d + O_d \\ f_{qv} = T_q + O_q + T_v + O_v \end{cases} \tag{25}$$

where T_d, T_q, T_v, O_d, O_q, O_v are the response time and overshoot of the d-axis current, the q-axis current, and the speed v, respectively.

V. SIMULATION AND ANALYSIS

The adaptive fitness curve of sliding mode control parameters using PSO is shown in Fig. 10. After optimization, enter the optimal control parameters into the sliding mode control strategy and the results are shown in Fig. 11.

According to Fig. 11, the sliding mode control rate designed in this paper can disengage the WEC from the chaotic state of a given target value. Following the sliding mode control strategy with PSO optimizing control parameter, WEC takes less time to disengage from chaotic state and reach steady state, the overshoot is suppressed, and the control effect is improved.

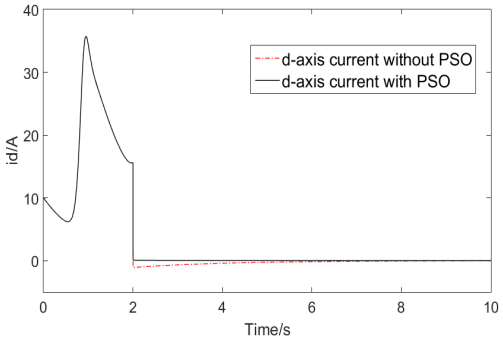

(a) d-axis current of WEC (Add control after 2s)

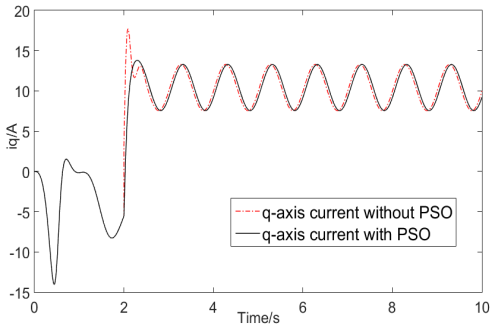

(b) q-axis current of WEC(Add control after 2s)

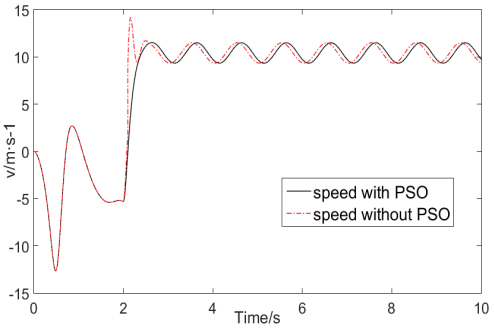

(c) speed of WEC(Add control after 2s)

FIGURE 11. Dynamic response of WEC under sliding mode control and optimized sliding mode control.

VI. CONCLUSION

By building the decoupling mathematical model, it is verified that the WEC may appear chaotic phenomenon during operation. A sliding mode controller is proposed to disengage the WEC from the chaotic state. BP neural network is adopted to fit the global control effect under different sliding mode control parameters. The PSO algorithm is employed to optimize the sliding mode control strategy and determine the optimal control parameters. The simulation indicates that the sliding mode control strategy can achieve the WEC chaos detachment and stability control. The sliding mode control strategy with PSO optimization can reduce the response time, suppress the overshoot, and improve the control effect and system robustness. In the subsequent work, more complex and actual marine environment, accurate WEC model, the chaotic characteristic of the entire wave energy generation system, how to suppress the sliding mode chattering and design improved control strategies may be considered.

REFERENCES

[1] C. Zheng, B. Jia, and S. Guo, "Wave energy resource storage assessment in global ocean," (in Chinese), *Resour. Sci.*, vol. 35, no. 8, pp. 1611–1616, 2013.

[2] Y. Yage, L. Wei, L. Weimin, L. Xiaoying, and W. Feng, "Development status and perspective of marine energy conversion systems," *Automat. Electr. Power Syst.*, vol. 34, no. 14, pp. 1–12, 2010.

[3] M. Prado and H. Polinder, "Direct drive in wave energy conversion—AWS full scale prototype case study," in *Proc. IEEE Power Energy Soc. General Meeting*, Jul. 2011, pp. 1–7.

[4] H. Polinder, B. C. Mecrow, A. G. Jack, P. Dickinson, and M. A. Mueller, "Conventional and TFPM linear generators for direct-drive wave energy conversion," *IEEE Trans. Energy Convers.*, vol. 20, no. 2, pp. 260–267, Jun. 2005.

[5] A. Shibaike, M. Sanada, and S. Morimoto, "Suitable configuration of permanent magnet linear synchronous generator for wave power generation," in *Proc. Power Convers. Conf.-Nagoya*, Apr. 2007, pp. 210–215.

[6] L. Chunyuan, Y. Haitao, H. Minqiang, Y. Qiang, and C. Zhongxian, "Application of permanent magnet tubular linear generators using direct-driver wave power generation take-off systems," *Proc. CSEE*, vol. 33, no. 21, pp. 90–98, 2013.

[7] L. Huang, M. Hu, Z. Chen, H. Yu, and C. Liu, "Research on a direct-drive wave energy converter using an outer-PM linear tubular generator," *IEEE Trans. Magn.*, vol. 53, no. 6, Jun. 2017, Art. no. 8104704.

[8] A. E. Elgebaly and M. K. El-Nemr, "Design and performance evaluation of Halbach array linear generator for wave energy converters," in *Proc. IEEE 8th GCC Conf. Exhib.*, Feb. 2015, pp. 1–6.

[9] H. Polinder, M. E. C. Damen, and F. Gardner, "Linear PM generator system for wave energy conversion in the AWS," *IEEE Trans. Energy Convers.*, vol. 19, no. 3, pp. 583–589, Sep. 2004.

[10] F. Wu, X. P. Zhang, and P. Ju, "Control strategy for AWS based wave energy conversion system," in *Proc. IEEE PES General Meeting*, Jul. 2010, pp. 1–2.

[11] F. Wu, P. Ju, X.-P. Zhang, C. Qin, G. J. Peng, H. Huang, and J. Fang, "Modeling, control strategy, and power conditioning for direct-drive wave energy conversion to operate with power grid," *Proc. IEEE*, vol. 101, no. 4, pp. 925–941, Apr. 2013.

[12] K. Qing, X. Xi, N. Zanxiang, H. Lipei, and S. Kai, "Design of grid-connected directly driven wave power generation system with optimal control of output power," in *Proc. 15th Eur. Conf. Power Electron. Appl. (EPE)*, Sep. 2013, pp. 1–8.

[13] H. M. Hasanien, "Transient stability augmentation of a wave energy conversion system using a water cycle algorithm-based multiobjective optimal control strategy," *IEEE Trans. Ind. Inform.*, vol. 15, no. 6, pp. 3411–3419, Jun. 2019.

[14] H. M. Hasanien, "Gravitational search algorithm-based optimal control of archimedes wave swing-based wave energy conversion system supplying a DC microgrid under uncertain dynamics," *IET Renew. Power Gener.*, vol. 11, no. 6, pp. 763–770, May 2017.

[15] Z. Wang and K. T. Chau, "Design, analysis, and experimentation of chaotic permanent magnet DC motor drives for electric compaction," *IEEE Trans. Circuits Syst. II, Exp. Briefs*, vol. 56, no. 3, pp. 245–249, Mar. 2009.

[16] X. H. Mai, D. Q. Wei, B. Zhang, and X. S. Luo, "Controlling chaos in complex motor networks by environment," *IEEE Trans. Circuits Syst. II, Exp. Briefs*, vol. 62, no. 6, pp. 603–607, Jun. 2015.

[17] Z. Li, J. B. Park, Y. H. Joo, B. Zhang, and G. Chen, "Bifurcations and chaos in a permanent-magnet synchronous motor," *IEEE Trans. Circuits Syst. I, Fundam. Theory Appl.*, vol. 49, no. 3, pp. 383–387, Mar. 2002.

[18] J. Sun, X. Zhao, J. Fang, and Y. Wang, "Autonomous memristor chaotic systems of infinite chaotic attractors and circuitry realization," *Nonlinear Dyn.*, vol. 94, no. 4, pp. 2879–2887, 2018. doi: 10.1007/s11071-018-4531-4.

[19] R. Yang, M. Wang, C. Zhang, and L. Li, "Robustness improvement of predictive current control for PMLSM integrating adaptive internal model with time delay compensation," in *Proc. 20th Int. Conf. Elect. Mach. Syst. (ICEMS)*, Aug. 2017, pp. 1–5.

[20] Q. He and Q. Wang, "Optimal design of low-speed permanent magnet generator for wind turbine application," in *Proc. Asia–Pacific Power Energy Eng. Conf.*, Mar. 2012, pp. 1–3.

[21] G. Kun, "A high speed chaos controller for modified coupled dynamos system," in *Proc. Int. Conf. Consum. Electron., Commun. Netw. (CECNet)*, Apr. 2011, pp. 4650–4653.

[22] R. Lina, L. Fucai, and J. Yafei, "Active disturbance rejection control for chaotic permanent magnet synchronous generator for wind power system," in *Proc. 31st Chin. Control Conf.*, Jul. 2012, pp. 6878–6882.

[23] C. Qiang, Y.-R. Nan, and K.-X. Xing, "Adaptive sliding-mode control of chaotic permanent magnet synchronous motor system based on extended state observer," *Acta Phys. Sinica*, vol. 63, no. 22, p. 220506, 2014.

[24] L. Hou, K. Cai, R. Li, and Z. Tian, "Nonsingular fast terminal-sliding-mode control of chaotic motion in PMSM based on speed sensorless," *Inf. Control*, vol. 45, no. 6, pp. 666–670, 2016.

[25] D. Xie, J. Yang, H. Cai, F. Xiong, B. Huang, and W. Wang, "Blended chaos control of permanent magnet linear synchronous motor," *IEEE Access*, vol. 7, pp. 61670–61678, 2018.

[26] Y. Soufi, S. Kahla, and M. Bechouat, "Particle swarm optimization based sliding mode control of variable speed wind energy conversion system," *Int. J. Hydrogen Energy*, vol. 41, no. 45, pp. 20956–20963, 2016.

[27] S. Junwei, W. Yan, W. Yanfeng, and S. Yi, "Finite-time synchronization between two complex-variable chaotic systems with unknown parameters via nonsingular terminal sliding mode control," *Nonlinear Dyn.*, vol. 85, no. 2, pp. 1105–1117, 2016.

[28] J. Sun, Y. Wu, G. Cui, and Y. Wang, "Finite-time real combination synchronization of three complex-variable chaotic systems with unknown parameters via sliding mode control," *Nonlinear Dyn.*, vol. 88, no. 3, pp. 1677–1690, 2017.

[29] H. Chaoui, M. Khayamy, and A. A. Aljarboua, "Adaptive interval type-2 fuzzy logic control for PMSM drives with a modified reference frame," *IEEE Trans. Ind. Electron.*, vol. 64, no. 5, pp. 3786–3797, May 2017.

[30] L. Jie and H.-P. Ren, "Partial decoupling control of chaos in permanent magnet synchronous motor," *Control Theory Appl.*, vol. 22, no. 4, pp. 637–640, 2005.

[31] E. N. Lorenz, "Deterministic nonperiodic flow," *J. Atmos. Sci.*, vol. 20, no. 2, pp. 130–141, 1963.

[32] E. N. Lorenz and R. C. Hilborn, "The essence of chaos," *Phys. Today*, vol. 63, no. 48, pp. 862–863, 1995.

[33] A. Wolf, J. B. Swift, H. L. Swinney, and J. A. Vastano, "Determining Lyapunov exponents from a time series," *Phys. D, Nonlinear Phenomena*, vol. 16, no. 3, pp. 285–317, 1985.

[34] H. Jiang, L. Yang, L. Lin, H. Ji, and D. Shan, "Optimal speed control system of generator based on chaotic particle swarm optimization," in *Proc. Int. Conf. Elect. Control Eng.*, Jun. 2010, pp. 1426–1429.

JUNHAO HUANG was born in Guangdong, China, in 1995. He received the B.S. degree in electrical engineering and automation from the Guangdong University of Technology, Guangzhou, China, in 2018, where he is currently pursuing the M.S. degree in electrical engineering.

His current research interests include chaotic phenomenon analysis and the control of wave power converters, and the control of new energy generation.

JUNHUA YANG was born in Henan, China, in 1965. He received the B.Sc. and Ph.D. degrees from the South China University of Technology, in 1985, 1991, and 2006, respectively. He is currently a Professor with the School of Automation, Guangdong University of Technology, Guangzhou.

His research interests include electrical appliances and their control, and new energy generation control.

DONGSHEN XIE was born in Guangzhou, China, in 1993. He received the B.S. degree in electrical engineering and automation from the Changchun University of Science and Technology, Changchun, China, in 2016. He is currently pursuing the M.S. degree in electrical engineering from the Guangdong University of Technology, Guangzhou.

His current research interests include chaotic phenomenon analysis and the control of linear motors, and the control of new energy generation.

DANQI WU was born in Guangzhou, China, in 1993. She received the B.S. degree in electrical engineering and its automation with the Guangdong University of Technology, Guangzhou, China, in 2016, where she is currently pursuing the M.S. degree in electrical engineering.

Her current research interests include smart grids, energy management systems, and electricity systems.